Packaging-Compatible High Q Microinductors and Microfilters for Wireless Applications

Jae Yeong Park, *Member, IEEE*, and Mark G. Allen, *Member, IEEE*

***Abstract*—To meet requirements in mobile communication and microwave integrated circuits, miniaturization of the inductive components that many of these systems require is of key importance. At present, active circuitry is used which simulates inductor performance and which has high Q-factor and inductance; however, such circuitry has higher power consumption and higher potential for noise injection than passive inductive components. An alternate approach is to fabricate integrated inductors, in which lithographic techniques are used to pattern an inductor directly on a substrate or a chip. However, integrated inductors can suffer from low Q-factor and high parasitic effects due to substrate proximity.**

To expand the range of applicability of integrated microinductors at high frequency, their electrical characteristics, especially quality factor, should be improved. In this work, integrated spiral microinductors suspended (approximately 60 μm) above the substrate using surface micromachining techniques to reduce the undesirable effect of substrate proximity on the inductor performance are investigated. The fabricated inductors have inductances ranging from 15–40 nH and Q-factors ranging from 40–50 at frequencies of 0.9–2.5 GHz. Microfilters based on these inductors are also investigated by combining these inductors with integrated polymer filled composite capacitors.

***Index Terms*—Electroplating, high Q inductors, integrated, LC passive filter, low temperature processes, polymer/metal multilayer processing, surface micromachining.**

I. Introduction

THERE are a large number of discrete passives and relatively fewer integrated circuits (IC's) required in many consumer electronic products such as VCR's, pagers, cellular phones, GPS receivers, and camcorders, and RF or mixed-signal systems. The impact of the large number of discrete passives on system cost, size, weight, and reliability is substantial. An approach to addressing these issues is integrating these passive components directly into a multichip module (MCM), IC chips, or other packaging substrates [1], [2]. In this research, fabrication technologies such as surface micromachining have been applied to fabricate integrated passive components with good performance characteristics at high frequency. The fabrication technologies are also compatible with conventional complementary metal-oxide-semiconductor (CMOS) processes.

Manuscript received March 27, 1998; revised January 29, 1999. This work was supported in part by the National Science Foundation through the Georgia Tech/NSF Engineering Research Center in Electronic Packaging under Contract EEC-9402723.

The authors are with the School of Electrical and Computer Engineering, Georgia Institute of Technology, Atlanta, GA 30332-0269 USA (e-mail: mark.allen@ece.gatech.edu).

Publisher Item Identifier S 1521-3323(99)03740-5.

Much research has been done to improve the performance characteristics of integrated inductors by reducing parasitics and loss from the substrate. Recent examples include air gap spiral inductor structures that have been fabricated using glass microbump bonding (GMBB) to reduce losses and parasitic capacitance [3]. Due to the presence of the air gap, the parasitic capacitance can be minimized, thereby enhancing the resonant frequency. A large suspended inductor on silicon for RF amplifier applications was fabricated in [4]; the deleterious effects of the silicon substrate were reduced by selectively etching out the silicon under the inductor. Transistor-integrated suspended spiral inductors formed from the metallization used in GaAs technologies have been produced; using air-bridge technologies, these devices have a typical air gap of 3 μm between the conductor lines which form the inductor and the substrates [5]. Solenoid-type inductors have also been produced using a combination of electroplating and micromachining techniques that are suspended approximately 20 μm above the substrate [6]. Examples of integrated passive filters incorporating integrated inductors have also been presented. A thin film LC passive filter has been fabricated by RF sputtering and ion-milling techniques [7]. A multilayer thin-film air core passives filter for the 850 MHz band was demonstrated in [8]. Other examples of integrated passive components based on MCM-C (ceramic) and MCM-D (deposited) technology are described in [9]–[11].

In this research, surface-micromachined suspended air core spiral inductors and passive LC filters based on these inductors are designed, fabricated, and characterized. Surface micromachining allows assessment of the feasibility of using various low cost substrates to fabricate integrated passives while maintaining good performance characteristics. The inductors have spiral geometry with an air core and a large air gap (60 μm height) between the coils and the substrate (to reduce substrate parasitics), and thick, highly conductive electroplated copper conductor lines (to increase the quality factor). Various inductor geometries are also investigated by designing and fabricating several inductors with differing core areas and numbers of turns.

To fabricate passives filters, integrated metal-insulator-metal (MIM) capacitors are implemented using dielectric composite as an insulator, and these capacitors are integrated with the suspended inductors. The most commonly used geometry for integrated capacitors consists of two parallel conductor plates separated by a high-dielectric-constant material. An example of a suitable high dielectric constant material that is consistent with low temperature processing is a cured

suspension of a high dielectric constant material suspended in an organic binder. Such polymer ceramic composites are a favorable choice for thin film capacitors in low temperature MCM-L or MCM-L/D technology [12], [13]. These dielectric materials are two-phase composites in which the polymer allows low temperature fabrication and the filler enhances the dielectric constant of the resulting composite far beyond that of the unfilled polymer. However, there are many other requirements for integration of these capacitors, such as the ability to form thin ($\sim$5 μm) uniform films with high dielectric constant (50–100 for many applications); tan delta $<$ 0.01; low temperature curing with high temperature stability; and good adhesion to a variety of substrates are of primary importance. In this work, polyimide organic binders filled with lead magnesium niobate particles were employed to fabricate integrated capacitors [12].

II. Design and Modeling

For high frequency applications, it is most appropriate to consider air-core inductor devices, since the high frequency behavior of many magnetic core materials is relatively poor. The characteristics of an integrated inductor with a nonmagnetic core can be determined solely by the coil geometry and location. In addition to accurate determination of the inductance of air-core inductors, it is also important at high frequency to assess parasitic effects such as stray capacitance and conductor skin effect in order to understand the effective operation of the device. Much research has been done to analyze the stray capacitance of an integrated inductor in high frequency applications [14]–[16]. The stray capacitance of the inductor determines the self-resonant frequency (SRF) and the Q-factor. Various aspects of the inductor geometry, such as the cross- sectional area of the conductor line, the line spacing, and the core size, must be considered such that the inductor has the desired performance after fabrication. The resistivity of the metal conductor should be low to obtain a high Q-factor at high frequency applications. Since high frequency current flows mostly along the surface area of a conductor, the skin effect causes the winding resistance to increase as the frequency is increased. Thicknesses of conductor lines much in excess of several skin depths at the frequency of interest will not greatly reduce the conductor resistance or increase the inductor Q-factor.

A spiral inductor design is considered for the realization of a high-Q integrated inductor due to its simplicity of fabrication as well as its large achievable core cross-sectional area. Fig. 1 shows a schematic drawing of an integrated spiral inductor with a large air gap between the conductor lines and the substrate. The air gap is maintained by plated copper metal supports that allow the air gap to be large compared with traditional air bridge approaches, thus reducing the stray capacitance from the substrate. Thick (e.g., electroplated) conductor lines (i.e., several skin depths) are also desirable to increase the cross-sectional area of the conductor and thereby reduce the conductor resistance.

Much research has been performed for modeling spiral inductors and predicting their inductance with and without consideration of parasitic effects [17]–[19]. As shown in (1), a square spiral inductor may be defined by the five independent geometric variables in free space [20]

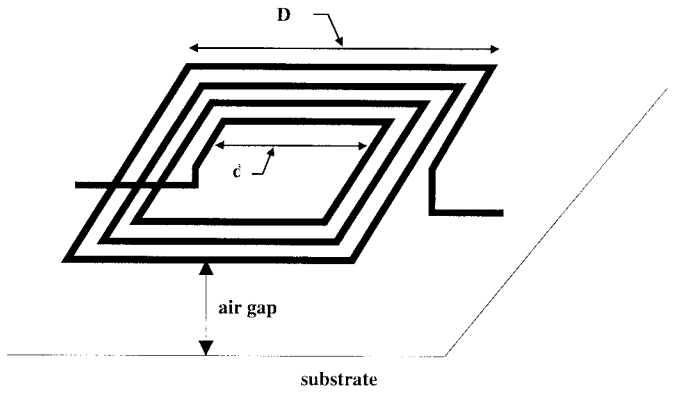

Fig. 1. Schematic drawing of the fabricated spiral-type air core inductor with a large air gap between the conductor lines and the substrate.

$$L = F(D+d,\, D-d,\, N,\, s,\, t) \tag{1}$$

where D and d are the outermost and innermost dimensions, respectively, as shown in Fig. 1; and N, s, and t are the number of turns, line spacing and metal thickness of the given square spiral inductor. Bryan found an empirical equation to calculate the inductance of a flat square spiral-type inductor based on these variables [19], [21]

$$L = 0.0241 a N^{(5/3)} \ln\left[8\left(\frac{a}{c}\right)\right] \tag{2}$$

where

$$a = \frac{D+d}{4}, \quad c = \frac{D-d}{2}. \tag{3}$$

Equation (2) predicts inductance in microhenries when dimensions are expressed in centimeters.

The unloaded Q-value is found by taking the ratio of the imaginary part to the real part of the input impedance of the inductor (neglecting bonding pads and interconnect) as shown in

$$Q_{unloaded} = \frac{\mathrm{Im}\{Z_{\mathrm{in}}\}}{\mathrm{Re}\{Z_{\mathrm{in}}\}}. \tag{4}$$

High quality factor means that the inductor has the desirable properties of low dissipation and favorable frequency characteristics when utilized in filter circuits. The effects of the substrate on the SRF and Q-factor can be reduced by introducing a large air gap between the substrate and the spiral coils. In the spiral geometry, this approach can also reduce winding capacitance by spatially separating the spiral coils from the central return lead. Such large air gaps can be achieved using a surface micromachining technique using, e.g., a polyimide sacrificial layer.

III. Fabrication of Microinductors and Microfilters

The fabricated LC passive filter is composed of a suspended spiral-type air core inductor supported by thick electroplated

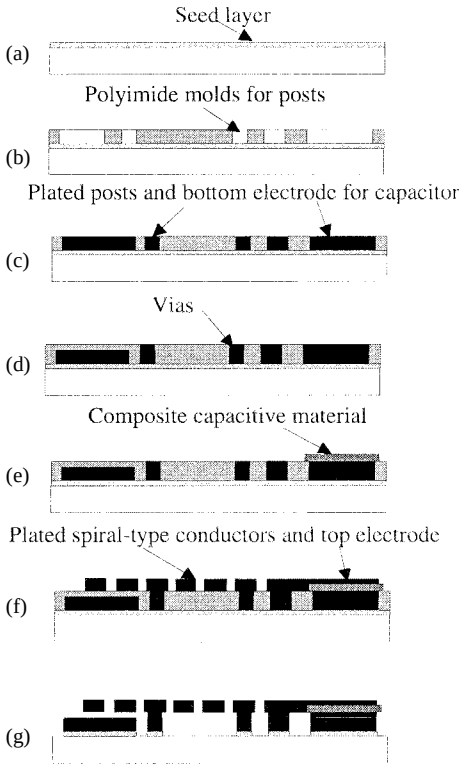

Fig. 2. Fabrication sequences of a large suspended spiral-type microinductor and a microfilter: (a) seed layer deposition, (b) formation of polyimide molds for posts and bottom electrodes for capacitors, (c) plating of posts and bottom electrodes for capacitors (copper), (d) via formation, (e) deposition of composite capacitive materials by spin casting, (f) formation of spiral type conductor lines and top electrode using electroplating techniques, and (g) removal of polyimide using plasma etcher and seed layer using wet-etching solutions.

copper metal posts, and an MIM high dielectric constant composite capacitor. In addition to integrated filter structures, test structures consisting of isolated inductors and isolated capacitors were also fabricated using the same lithographic mask set. Fig. 2 shows the fabrication sequence of the integrated LC filter using spiral-type air core inductors and composite MIM capacitors. A Ti/Cu/Ti seed layer was deposited on the glass substrate and polyimide (Dupont PI-2611) was then coated on top of the deposited seed layer to build electroplating molds for posts, test pads, and grounds. A conventional low-cost glass substrate, with no optimization of glass properties for high frequency operation, was used as the starting material. Two coats were applied to obtain 15 μm thick polyimide molds. Each coat was cast at 600 rpm for 20 s, 3500 rpm for 4 s, and soft-baked at 120 °C in a convection oven for 10 min prior to the application of the next coat. After spin-casting all coats, the polyimide was hard-cured at 200 °C for 0.5 h and 300 °C for 1 h in nitrogen. The polyimide molds were formed using plasma O_2 etch and an aluminum hard mask. The electroplating molds were then filled with copper using standard electroplating techniques. Two coats of polyimide on top of the plated copper metal were spun and hard-cured. Electroplating molds were formed for a bottom electrode for the capacitor and via connections between selected posts and spiral- type conductor lines. The electroplating forms were then filled with copper using standard electroplating techniques. At this point, two

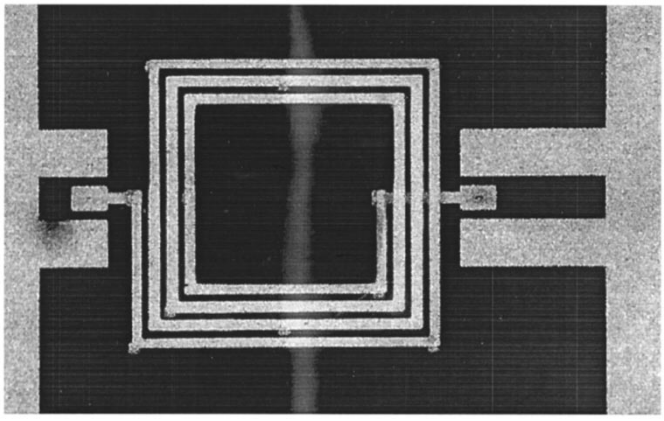

Fig. 3. Photomicrograph of the fabricated large suspended spiral-type air core inductor.

parallel fabrication paths were followed. To make integrated inductors alone, a seed layer (Ti/Cu/Ti) was then deposited and 15 μm thick photoresist was coated on the seed layer and patterned to form electroplating molds for conductor lines of the inductors. The electroplating molds were again filled with copper using standard electroplating techniques. The photoresist molds were then removed and the seed layer wet-etched. Plasma etching using 80% O_2 and 20% CHF_3, was used to remove all polyimide on top of the substrate. After removing all polyimide, the bottom seed layer was wet-etched. To make integrated filters, composite dielectric material (Dupont 2721 photosensitive polyimide filled with lead magnesium niobate powder) was then spin-coated at 600 rpm for 10 s and 4000 rpm for 60 s continuously. The coated dielectric films were soft cured, exposed through a mask, developed, and hard cured at 300 °C for 1 h in nitrogen. A seed layer (Ti/Cu/Ti) was then deposited and 15 μm thick photoresist was coated on the seed layer and patterned to form electroplating molds for top electrodes of the MIM capacitors and conductor lines of the inductors. The electroplating molds were again filled with copper using standard electroplating techniques. The photoresist molds were then removed and the seed layer wet-etched. Plasma etching using 80% O_2 and 20% CHF_3, was used to remove all polyimide on top of the substrate. The addition of the CHF_3 gas also facilitated the removal of the polyimide under the metal conductor lines. After removing all polyimide, the bottom seed layer was wet-etched. Figs. 3 and 4 show optical and SEM photomicrographs of the fabricated suspended spiral-type air core inductor. Fig. 5 shows a side view of the fabricated large suspended spiral-type air core inductor. Fig. 6 shows a scanning electron micrograph of large suspended (approximately 60 μm) plated spiral conductor lines and signal connection through a plated via. Fig. 7 shows a photomicrograph of a fully integrated RF-LC filter using composite MIM capacitor and spiral-type air core inductor suspended over the substrate (dimension: 1.9 mm $\times$ 2.4 mm).

IV. Experimental Results and Discussions

Following many of the procedures in [22], the fabricated spiral-type air core microinductors as well as an LC passive

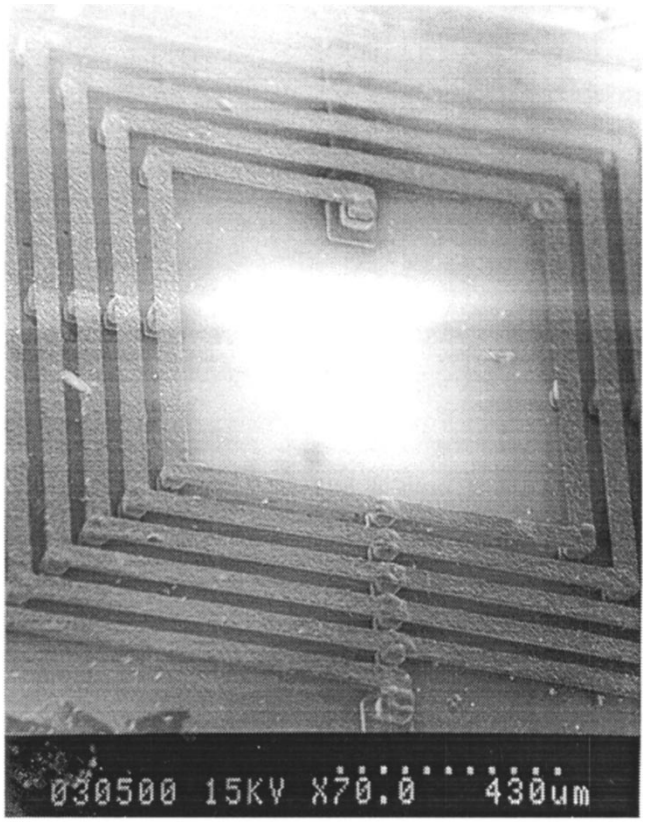

Fig. 4. Scanning electron micrograph of the fabricated large suspended spiral-type air core inductor.

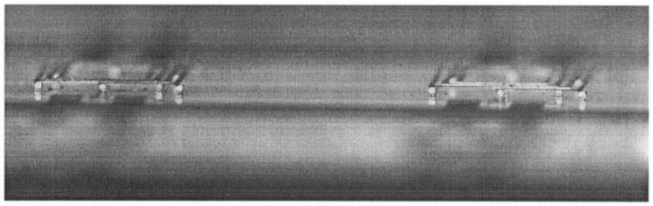

Fig. 5. Side view of the fabricated large suspended spiral-type air core inductor.

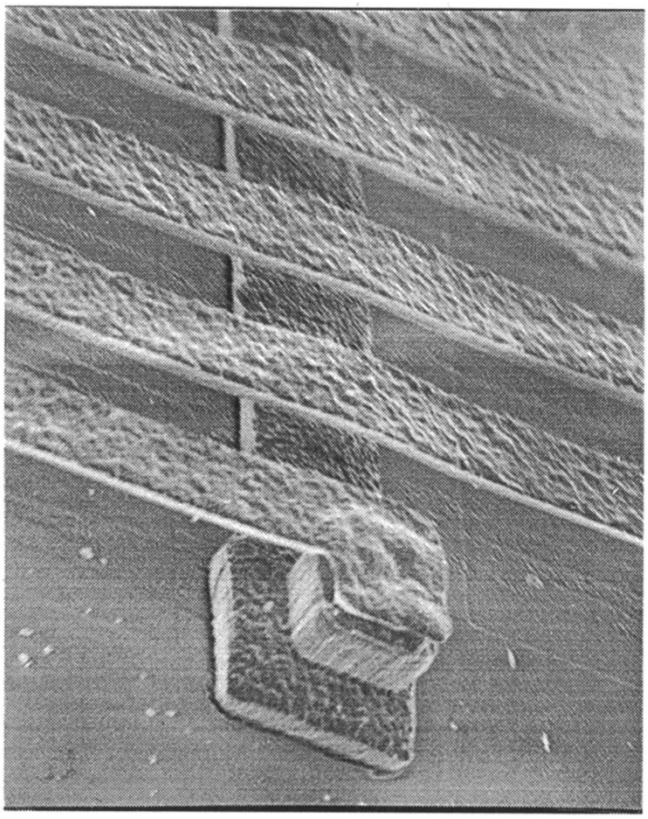

Fig. 6. Scanning electron micrograph of large suspended plated spiral conductor lines and signal connection through plated via (all metals are plated copper).

microfilter composed of a spiral-type air core inductor and a composite MIM capacitor, were measured. The experimental setup was an HP 85109C network analyzer, and CASCADE MICROTECH ground-signal-ground high frequency coplanar probes with 150 μm pitch size. After calibration on open, short, and 50 Ω resistor standards, the measurement was performed. In this measurement, the parasitics of the probe pads were not de-embedded. The measured two-port S-parameters were transformed into one-port S-parameters by terminating one of the ports with ground at an HP microwave and RF design system (MDS). A reflection coefficient, S_{11} of the transformed one-port S parameters was translated into an input impedance, Z_{in} for evaluating inductance and quality factor of fabricated inductors using the MDS tool. The unloaded Q-factor was determined by dividing the imaginary part of the input impedance Z_{in} by the real part (dissipated energy). The inductance was computed by dividing the imaginary part of the input impedance (inductive stored energy) by the frequency ω under the assumption that the effect of the parasitic capacitance in these structures at frequencies much lower than the self-resonant frequency is small. The characteristics of the integrated filter were determined by analyzing the measured scattering matrix. For measurement of the integrated filter, an HP 8510 network analyzer was used. The magnitude of the transmission coefficient S_{21} is the gain, and $\arg S_{21}$ is the phase difference between the input and output ports of the fabricated microfilter.

Table I shows a list of the different geometries of the fabricated spiral-type air core microinductors. These inductors have 40-μm-wide and 9-μm-thick electroplated copper conductor lines, and the spacing between the windings is 40 μm. All inductors are suspended over the substrate by approximately 60-μm air gaps. The actual thickness of the copper conductor lines after completing fabrication was 9 μm. The measured dc resistance of the fabricated inductors is well matched with calculated values based on the length and measured thickness of conductor lines and the resistivity of electroplated copper. Figs. 8 and 9 show a comparison of inductance and quality factor as a function of frequency of the fabricated spiral-type air core inductors. As shown in Fig. 8, as both the number of turns and core area are increased, the inductance is increased as predicted. However, as frequency is increased, the inductors with large number of turns produce lower quality factor and self-resonant frequency, since the longer conductor lines produce higher series resistance and parasitic capacitance. At higher frequencies, shorter conductor

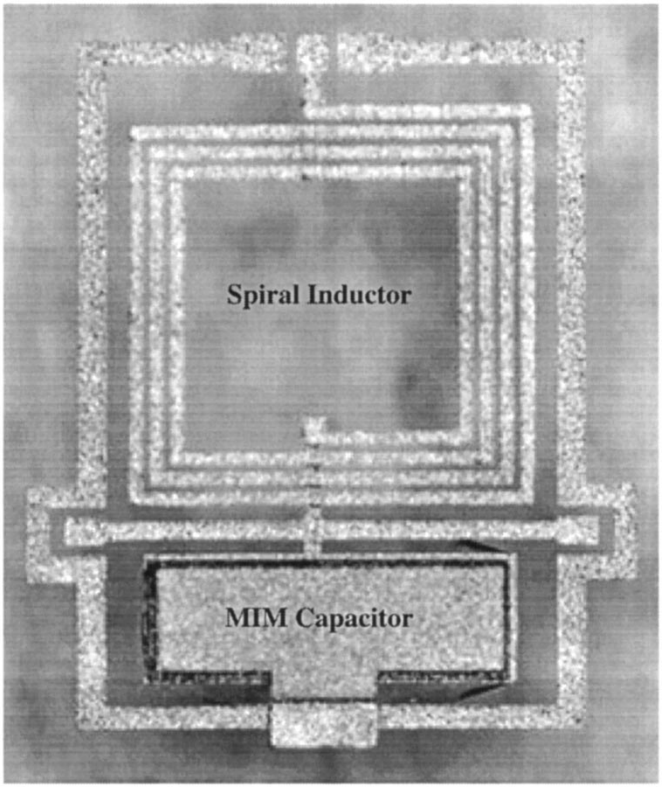

Fig. 7. Photomicrograph of fully integrated RF-LC filter using composite MIM capacitor and spiral-type air core inductor suspended over the substrate (dimension: 1.9 mm × 2.4 mm).

TABLE I
DESIGNED PARAMETERS OF THE FABRICATED LARGE SUSPENDED SPIRAL-TYPE AIR CORE INDUCTOR

Type	Dimension of fabricated inductors (mm)	Width, thickness, and spacing of conductor lines (μm)	Core area (mm)	Number of turns
A	1.28 x 1.28	40 x 9 x 40	0.8 x 0.8	3.5
B	1.3 x 1.3	40 x 9 x 40	0.5 x 0.5	5.5
C	1.03 x 1.03	40 x 9 x 50	0.5 x 0.5	3.5

lines and larger core area are required to have higher quality factor and self-resonant frequency (SRF). In the comparison of these fabricated inductors, the A-type inductor has the maximum Q-value, 50 at 0.8 GHz with an SRF of 2.85 GHz. The B-type inductor has a Q-value of 44 at 1.2 GHz with an SRF of 2.4 GHz, and the C-type inductor has a Q of 46 at 2.1 GHz with an SRF of 4.2 GHz.

Fig. 10 shows an equivalent circuit for the fabricated spiral-type inductor [23]. In the circuit, L models the self and mutual inductance in the spiral-type conductor lines, r is the series resistance, and C1 and C2 model the parasitic capacitance from the conductor lines and the substrate. In the circuit model, substrate resistance is not present because the glass substrate acts as the dielectric layer. The inductance and resistance of the inductor increase as operating frequency increases due to the skin effect of the conductor lines. The values of parameters of the equivalent circuits shown in Fig. 10 were obtained by non- linear fitting using an HP microwave and RF design system (MDS) tool. The equivalent inductor model was implemented in the MDS simulator that provides computer

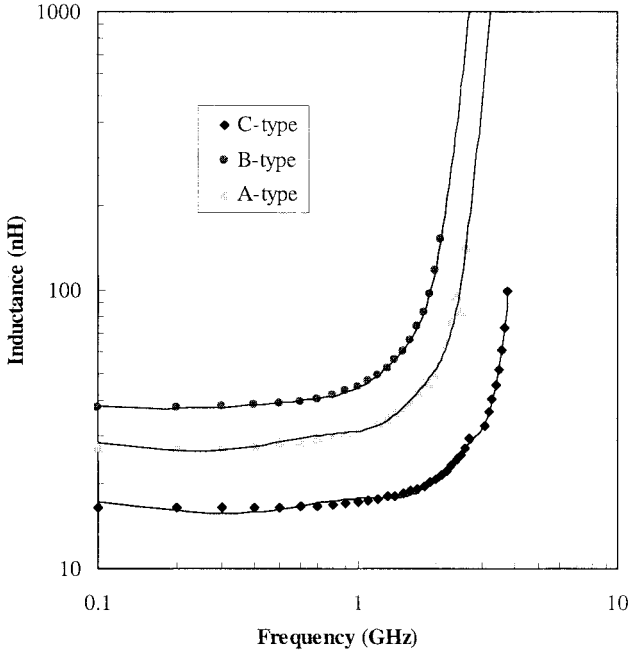

Fig. 8. Comparison of inductance of the fabricated spiral-type air core inductors suspended from the substrate.

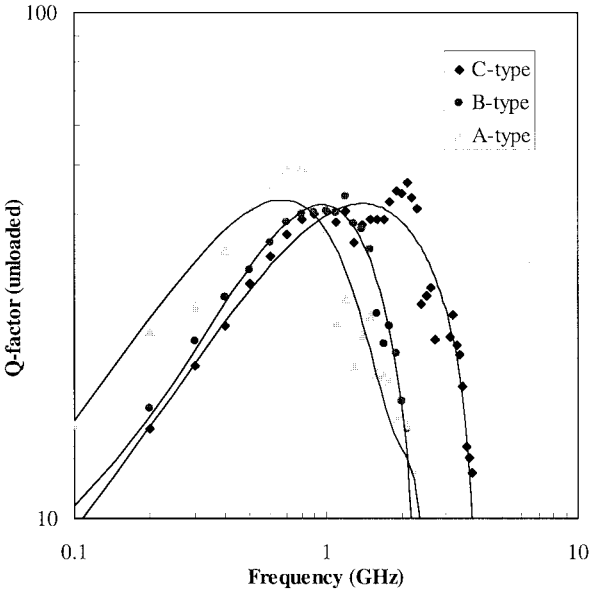

Fig. 9. Comparison of quality factor of the fabricated spiral-type air core inductors suspended from the substrate.

optimization for the fitting of the model parameters to the measured data. Table II shows the fit values of the equivalent circuit parameters obtained by the MDS simulator. As shown in Table II, the parasitic capacitance, C1 and C2 are slightly different, since the structure of the fabricated inductor is not symmetrical. A comparison of the measured and simulated S-parameters agree well up to a few GHz, with a slight discrepancy as frequency increases above several GHz.

Table III shows a comparison of the measured low frequency inductance and the analytically calculated inductance of the fabricated suspended air core spiral inductors. The calculated inductance was evaluated using (3) and (4). The

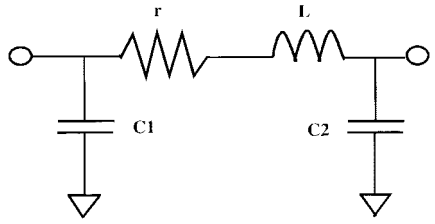

Fig. 10. Lumped element equivalent circuits for the fabricated large suspended spiral-type air core inductor.

TABLE II
COMPARISON OF MEASURED AND CALCULATED INDUCTANCE OF THE FABRICATED LARGE SUSPENDED SPIRAL-TYPE AIR CORE INDUCTOR

Type	Inductance, L (nH)	Resistance, r (ohms)	Capacitance, C1 (pF)	Capacitance, C2 (pF)
A	26.74	1.144	0.092	0.093
B	35.8	2.76	0.12	0.14
C	16	1.459	0.089	0.092

TABLE III
THE FITTING PARAMETERS OF LUMPED ELEMENT EQUIVALENT CIRCUITS FOR THE FABRICATED LARGE SUSPENDED SPIRAL-TYPE AIR CORE INDUCTOR

Type	Measured inductance (nH)	Calculated inductance (nH)	Measured self resonant frequency (GHz)
A	27.3	28.7	2.85
B	37.8	40.8	2.4
C	16.5	18.2	4.2

calculated inductance was slightly higher than the measured inductance. As the size of the inductor was reduced, the discrepancy between the measured inductance and the calculated inductance using Bryan's method increased. The C-type inductor that has the smallest size has the highest difference between measured and calculated inductance.

To demonstrate these integrated inductors in an application, an integrated passives filter composed of a spiral-type air core inductor and a MIM composite capacitor was fabricated and measured. The inductor is 1.5 mm $\times$ 1.5 mm in size, 40 μm in width, and 15 μm in conductor line thickness, with 40 μm spacing between conductor lines, and 3.5 turns of windings. The integrated capacitor is 0.3 mm $\times$ 1.2 mm in size. Fig. 11 shows the gain characteristics derived form the measured S-parameters of the fabricated LC filter. The fabricated filter is clearly a low pass filter with 3 dB attenuation at 880 MHz as shown in Fig. 11. The simulation of the fabricated filter was performed using the HP microwave and RF design system (MDS) tool by adding the measured capacitance value of the output capacitor, 2 pF at 100 kHz, into the measured S-parameters of the integrated inductor. The measured gain characteristic is slightly different than the simulated results as frequency is increased, since the parasitic capacitance of the interconnection and capacitor was excluded during the simulation.

V. CONCLUSION

Suspended integrated spiral microinductors with air core for wireless applications have been proposed, fabricated, and characterized using low temperature processes, electroplating techniques, and surface micromachining techniques. A 60 μm air gap was introduced between the spiral-type conductor lines and the substrate to achieve higher Q-value and self-resonant frequency by reducing substrate loss and the parasitic capacitance from the substrate which is dominant in the total parasitic capacitance. The air gap was realized by supporting the spiral-type conductor lines using plated copper posts at the edges and at the center of the conductor lines.

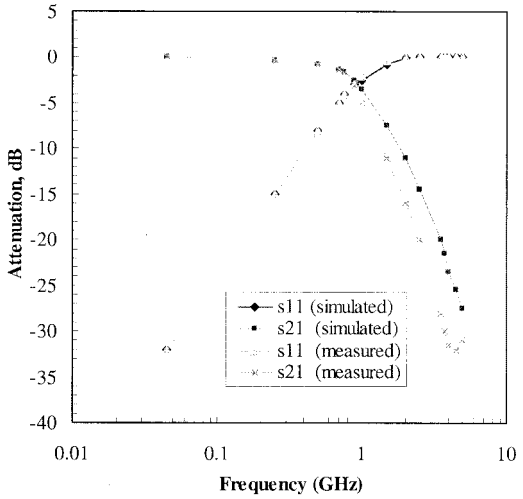

Fig. 11. Characteristics of the fabricated LC microfilter: 3 dB attenuation at 880 MHz.

Fabricated inductors with various geometries have been compared. As the number of turns is increased, the inductance, resistance, and parasitic capacitance are also increased. The increased resistance and parasitic capacitance reduce the Q-factor and the self-resonant frequency. These high Q integrated inductors are useful for communications, signal processing, MMIC circuitry, and analog circuitry applications operating at several GHz frequency ranges. A fully integrated LC filter with an air core spiral-type inductor and a MIM capacitor was also presented. The geometry and processing technology for integrated microinductors and microfilters show promise for application in systems operating in the several GHz region.

ACKNOWLEDGMENT

The authors would like to thank the Microsensor and Microactuator (MSMA) Group and Microelectronics Research Center staff for their help with processing questions, Dr. S. K. Bhattacharya, Packaging Research Center, Georgia Tech, for assistance with making of high dielectric composite materials for integrated capacitors, Dr. Y. J. Kim, Samsung Electronics, for valuable technical discussions and assistance, J. Laskar, Georgia Tech, and S. D. Senturia and M. Varghese, Massachusetts Institute of Technology, for their assistance.

REFERENCES

[1] J. Park and M. Allen, "Low temperature fabrication and characterization of integrated packaging-compatible, ferrite-core magnetic devices," in *Proc. IEEE 12th Appl. Power Electron. Conf.*, 1997, pp. 361–367.

[2] ——, "Packaging-compatible microinductors and microtransformers with screen-printed soft ferrite using low temperature processes," in *Proc. IEEE 7th Int. Joint MMM-Intermag Conf.*, 1998.

[3] J. Chuang, S. Ghazaly, N. Zein, G. Maracas, and H. Gronkin, "Low loss air-gap spiral inductors for MMIC's using glass microbump bonding techniques," in *Proc. IEEE-MTT-S Int. Microwave Symp. Dig.*, 1998, vol. 2, pp. 131–133.
[4] J. Y. C. Chang, A. A. Abidi, and M. Gaitan, "Large suspended inductors on silicon and their use in a 2 μm CMOS RF amplifier," *IEEE Electron Devices Lett.*, vol. 14, May 1993.
[5] M. E. Goldfarb and V. K. Tripathi, "The effect of air bridge height on the propagation characteristics of the microstrip," *IEEE Microwave Guided Wave Lett.*, vol. 1, pp. 273–274, Oct. 1991.
[6] Y. J. Kim and M. G. Allen, "Surface micromachined solenoid inductors for high frequency applications," *IEEE Trans. Comp., Packag., Manufact. Technol. C*, vol. 21, pp. 26–33, Jan. 1998.
[7] M. Yamaguchi, K. Ishihara, and K. Arai, "Application of thin-film inductors to LC filters," *IEEE Trans. Magn.*, vol. 29, no. 6, pp. 3222–3225, 1993.
[8] V. Sadhir, I. Bahl, and D. Willems, "CAD compatible accurate models of microwave passive lumped elements for MMIC applications," *Int. J. Microwave Millim.-Wave Comput.-Aided Eng.*, vol. 4, no. 2, pp. 148–162, 1994.
[9] R. Frye, K. Tai, M. Lau, and A. Lin, "Low-cost silicon-on-silicon MCM's with integrated passive components," in *Proc. 1992 Int. Electron. Packag. Conf.*, 1992, vol. 1, p. 343.
[10] R. Brown, A. Shapiro, and P. Polinski, "The integration of passive components into MCM's using advanced low temperature co-fired ceramics," *Int. J. Microcirc. Packag.*, vol. 16, no. 4, pp. 328–338, 1993.
[11] P. McCaffrey, "Integrated passive components for silicon hybrid multichip modules," in *Proc. Int. Electron. Packag. Conf.*, 1990, pp. 411–420.
[12] P. Chahal, R. Tummala, and M. Allen, "Novel integrated decoupling capacitor for MCM-L technology," *IEEE Trans. Comp., Packag., Manufact. Technol. B*, vol. 2, pp. 184–193, May 1998.
[13] D. K. Das-Gupta and K. Doughty, "Polymer/ceramic composite materials with high dielectric constant," *Thin Solid Films*, vol. 158, pp. 93–105, 1988.
[14] A. Massarini, M. Kazimierczuk, and G. Grandi, "Lumped parameter models for single- and multiple-layer inductors," in *Proc. 27th Annu. IEEE Power Electron. Specialists Conf.*, 1996, vol. 1, pp. 295–301.
[15] G. Grandi, M. Kazimierczuk, A. Massarini, and U. Reggiani, "Stray capacitances of single-layer air-core inductors for high-frequency applications," in *Proc. IAS'96, IEEE Ind. Applicat. Conf.*, 1996, vol. 3, pp. 1384–1388.
[16] B. Breen, "Multilayer inductor for high frequency applications," in *Proc. 41st Electron. Comp. Technol. Conf.*, 1991, pp. 551–554.
[17] D. Cahana, "A new transmission line approach for designing spiral microstrip inductors for microwave integrated circuits," in *IEEE-MTT-S Int. Microwave Symp. Dig.*, 1983, pp. 245–247.
[18] W. O. Camp, S. Tiwari, and D. Parson, "2–6 GHz monolithic microwave amplifier," in *IEEE-MTT-S Int. Microwave Symp. Dig.*, 1983, pp. 46–49.
[19] H. M. Greenhouse, "Design of planar rectangular microelectronic inductors," *IEEE Trans. Parts, Hybrids Packag.*, vol. PHP-10, pp. 101–109, June 1974.
[20] P. Li, "A new closed form formula for inductance calculation in microstrip line spiral inductor design," *Elect. Performance Electron. Packag.*, pp. 58–60, 1996.
[21] H. Bryan, "Printed inductors and capacitors," *Tele-Tech Electron. Ind.*, p. 68, 1955.
[22] I. Bahl, G. Lewis, and J. Jorgenson, "Automatic testing of MMIC's wafers," *Int. J. Microwave Millim.-Wave Comput.-Aided Eng.*, vol. 1, pp. 77–89, 1991.
[23] N. Nguyen and R. Meyer, "Si IC-compatible inductors and LC passive filters," *IEEE J. Solid-State Circuits*, vol. 25, no. 4, pp. 1028–1031, 1990.

Jae Yeong Park (S'94–M'96) received the M.S.E.E. and Ph.D. degrees in electrical and computer engineering from the Georgia Institute of Technology, Atlanta, in 1995 and 1997, respectively.

He is a Research Scientist with the School of Electrical and Computer Engineering, Georgia Institute of Technology. His research interests include the development, design, fabrication, and characterization of microsensors and microactuators; microstructures and technologies microelectromechanical systems (MEMS) compatible with IC fabrication; developing magnetic materials and deposition methods for micromagnetic devices such as electroplating and screen-printing; planar magnetic microinductors and microtransformers for wireless communications, power supplies (power converters and control circuits), and multichip modules; micromachined relays and switches; micromachined fluxgate sensors; and micromachined motors, etc.

Dr. Park is a member of IMAPS.

Mark G. Allen (M'89) received the B.A. degree in chemistry, the B.S.E. degree in chemical engineering, and the B.S.E. degree in electrical engineering from the University of Pennsylvania, Philadelphia, in 1984, and the S.M. and Ph.D. degrees in microelectronic materials from the Massachusetts Institute of Technology (MIT), Cambridge, MA, in 1986 and 1989, respectively.

His research at MIT focused on micromachining techniques to create structures for the *in-situ* measurement of mechanical properties and adhesion of thin films for use in microelectronic processing. He was also engaged in microsensors, microactuators, and in feedback-stabilized micromachined mirrors for laser applications. He joined the faculty of the Georgia Institute of Technology after a postdoctoral appointment at the Massachusetts Institute of Technology. His current research interests are in the field of micromachining and in microsensor and microactuator fabrication that is compatible with the IC fabrication. Other interests are in micromachined pressure and in acceleration sensors, micromotors, in integrated flow valves, in piezoelectric materials combined with semiconductor circuits and optical materials, in multichip packaging for integrated circuits and microstructures, in integration of organic piezoelectric materials with semiconductor circuits for sensing and actuation, and in materials and mechanical property issues in micromachining.

Dr. Allen is a member of the Editorial Board of the *Journal of Micromechanics and Microengineering*.